Pion scattering to collective excitations in ^{90}Zr and ^{118}Sn

J. L. Ullmann, P. W. F. Alons, B. L. Clausen, J. J. Kraushaar, J. H. Mitchell, R. J. Peterson, and R. A. Ristinen
Nuclear Physics Laboratory, Department of Physics, University of Colorado, Boulder, Colorado 80309

R. L. Boudrie, N. S. P. King, and C. L. Morris
Los Alamos National Laboratory, Los Alamos, New Mexico 87545

J. N. Knudson
Arizona State University, Tempe, Arizona 85284
and Los Alamos National Laboratory, Los Alamos, New Mexico 87545

E. F. Gibson
Physics Department, California State University, Sacramento, California 95819
(Received 7 August 1986)

Inelastic scattering of 163 MeV π^- and π^+ to the collective states of ^{90}Zr and ^{118}Sn was used to determine the neutron-proton composition of the transitions. The lowest 2^+ and 3^- states were examined for both targets, as were the low-energy octupole, giant quadrupole, and giant monopole excitations. Only slight deviations from the features expected for a hydrodynamic model are observed for the low-lying 3^- and 2^+ states of ^{118}Sn, but these states are observed to be proton-like in ^{90}Zr. The giant quadrupole resonances and giant monopole resonances in both targets show a significantly greater π^- than π^+ strength, while the low-energy octupole resonance is excited symmetrically.

I. INTRODUCTION

In recent investigations of the giant resonances in nuclei by inelastic pion scattering, some interesting and unexplained results have been obtained. Ullmann *et al.*[1] found that at a pion energy of 130 MeV the ratios of the inelastic π^- to π^+ cross sections for the excitation of the isoscalar giant quadrupole (GQR) and monopole (GMR) resonances in ^{118}Sn were 1.9 ± 0.4 and 2.3 ± 0.5, respectively. These values are considerably larger than predicted by the standard hydrodynamical model, which assumes equal neutron and proton vibrations. In this same study[1] it was shown that the cross-section ratios for the low-energy octupole resonance (LEOR) and the lower-lying collective states were nearly as expected from a hydrodynamic model. Subsequently, Seestrom-Morris *et al.*[2] found in a similar study at 162 MeV a value of $d\sigma(\pi^-)/d\sigma(\pi^+)$ for the GQR in ^{208}Pb of 2.72, which is far greater than the hydrodynamical model prediction.

The present study is an effort to obtain additional information on this effect by investigating ^{90}Zr, which has a smaller value of N/Z and a closed neutron shell, and by reinvestigating ^{118}Sn, which has a closed proton shell. In this study an incident pion energy of 163 MeV was chosen, which is closer to the (3,3) resonance than the 130 MeV previously used.

In a more general sense, inelastic π^+ and π^- scattering at 163 MeV can be extremely useful in determining the isoscalar and isovector contributions to the low-lying collective states or the giant collective modes. At this energy, the π^+-p interaction dominates that for π^+-n, and the converse is true for π^-. When restated in terms of isospin sensitivity, the sum or difference of π^- and π^+ scattering cross sections reveals the isoscalar or isovector scattering strengths, including their relative sign. To investigate this in more detail, we performed calculations using the distorted wave impulse approximation and collective model nuclear transition densities for comparison to the measured cross sections. The two pion charge states both show the same surface absorption features, and the same theoretical analyses were used for both. Moreover, the same experimental apparatus was used for both π^+ and π^-. Therefore the present study is a very consistent means to study the isoscalar and isovector amplitudes for the transitions.

Our results for the inelastic transition strengths are compared to those from other probes. Inelastic alpha-particle scattering is also strongly localized to the nuclear surface, and has been assumed to excite only the isoscalar mode. Electromagnetic transitions probe the entire nuclear volume but excite only the proton component of the transition. We make specific use of this property by using proton transition densities derived from electron scattering data to predict pion cross sections for ^{90}Zr in a model-independent fashion.

We present results for the lowest 2^+ and 3^- states and for the isoscalar low-energy octupole resonance (LEOR), isoscalar quadrupole resonance (GQR), and the nominal isoscalar monopole resonance (GMR), in both ^{90}Zr and ^{118}Sn at 163 MeV.

II. METHODS

A. Experimental methods

The data were taken on the EPICS facility at the Clinton P. Anderson Meson Physics Facility (LAMPF) of Los Alamos National Laboratory. Many of the experimental

details were as described in our earlier work.[1] Three targets were positioned in the same beam spot, with the reconstructed position of each event on the target plane used to select the histogram into which the spectra were binned. The targets were ^{118}Sn (enriched to 97% and 144 mg/cm^2 thick) and ^{90}Zr (enriched to 97.7% and in two sheets, 257 and 406 mg/cm^2 thick). The ^{90}Zr data presented here use only the thinner ^{90}Zr target. Normalization data were taken on CH_2 targets cut to the same strip shapes as the actual targets. Target angles were set at half the scattering angle.

The nominal channel beam energy of 164 MeV has been found by recent magnetic field measurements to be 163.5 MeV. After energy loss in the target, the average scattered energy was 163.1 MeV for the central ray. The range of beam energies in the dispersed spot on the target was determined by the channel transmission, $\Delta p/p = 2\%$.

Data were taken at two spectrometer central momentum settings to emphasize either the low-lying or the giant states. The spectrometer higher field setting was primarily for the low-lying states, but since this field placed a 13.2 MeV excitation at the center of the focal plane, giant resonance data were also obtained, albeit with fewer counts than for the longer runs with the lower field setting. Sample spectra are shown as Figs. 1 and 2.

A focal-plane muon-rejection circuit[3] was used to veto muon events that contribute a uniform background at high excitations. This improvement over our earlier work[1] permitted use of a higher pion beam energy. Additional muon rejection was provided by redundant time-of-flight determinations between a plastic scintillator at the entrance to the spectrometer and the trigger scintillator in the focal plane. The front scintillator degraded the energy resolution somewhat.

The elastic scattering cross sections were measured for the optical-model checks described below. The background for the low-lying states was taken to be linear in form and all extracted peaks were fit simultaneously with a fixed line shape. The line shape for the ^{118}Sn state was determined by fitting the elastic and 1.23-MeV states together, with an observed resolution of 250 keV (FWHM). This combined fitting was necessary due to the long tail on the elastic peak. In ^{90}Zr the line shape was obtained by fitting the elastic peak alone, with a resolution of 310 keV due to the thicker target. Some representative fits to the peaks of interest are shown in Fig. 1.

Sample high excitation spectra at 21 deg are shown in Fig. 2. Peak areas over an assumed straight-line continuum were extracted by fitting two Gaussian peaks, corresponding to the isoscalar giant quadrupole resonance (GQR) and the dipole/isoscalar-monopole region. The locations and widths of these were fixed from α-scattering experiments.[4] For ^{90}Zr these were as follows: GQR—$E_x = 14$ MeV, $\Gamma = 3.4$ MeV; monopole—$E_x = 16.2$ MeV, $\Gamma = 3.5$ MeV. For ^{118}Sn, GQR—$E_x = 13.2$ MeV, $\Gamma = 3.8$ MeV; monopole—$E_x = 15.5$ MeV, $\Gamma = 4.4$ MeV. At 21 deg, the location and width of one peak were varied while keeping the other parameters fixed. In all cases, the above adopted parameters were at or near the fitted chi-squared minimum. A major source of uncertainty in extracting a giant resonance peak area is the choice of the underlying continuum, which we assumed to be a straight line. We estimated this uncertainty by varying the background between maximum and minimum reasonable levels and took

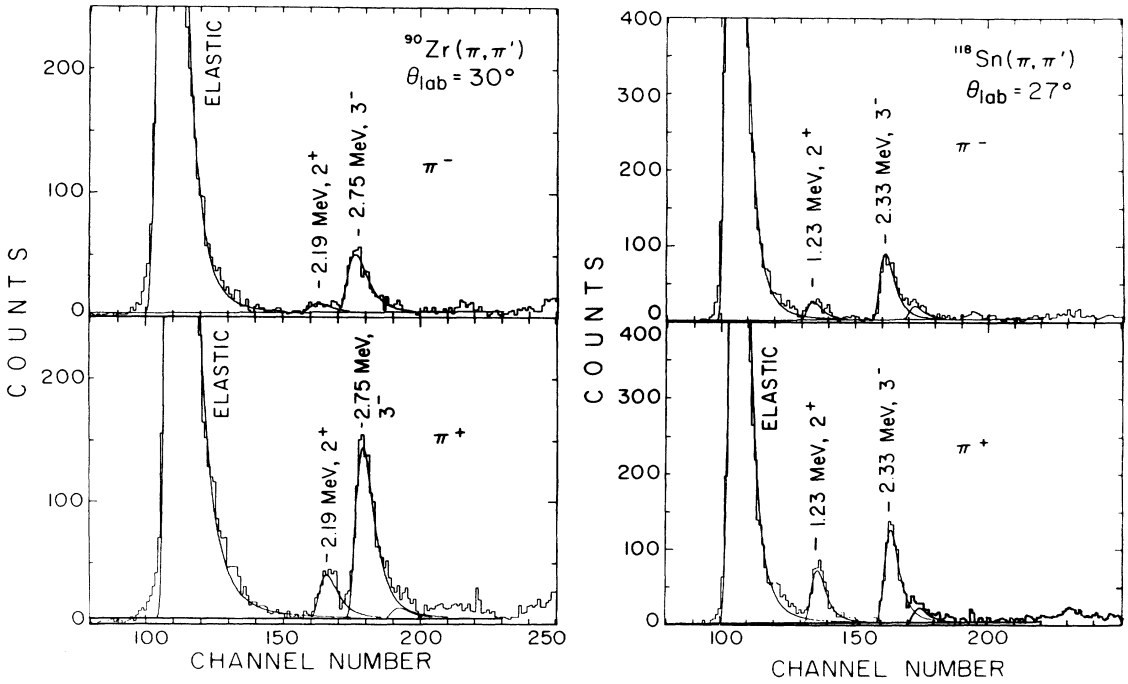

FIG. 1. Pion spectra for the low-lying collective excitations of ^{90}Zr and ^{118}Sn at a beam energy of 163 MeV. Skewed Gaussian shapes taken from the elastic peak are used for the known peaks.

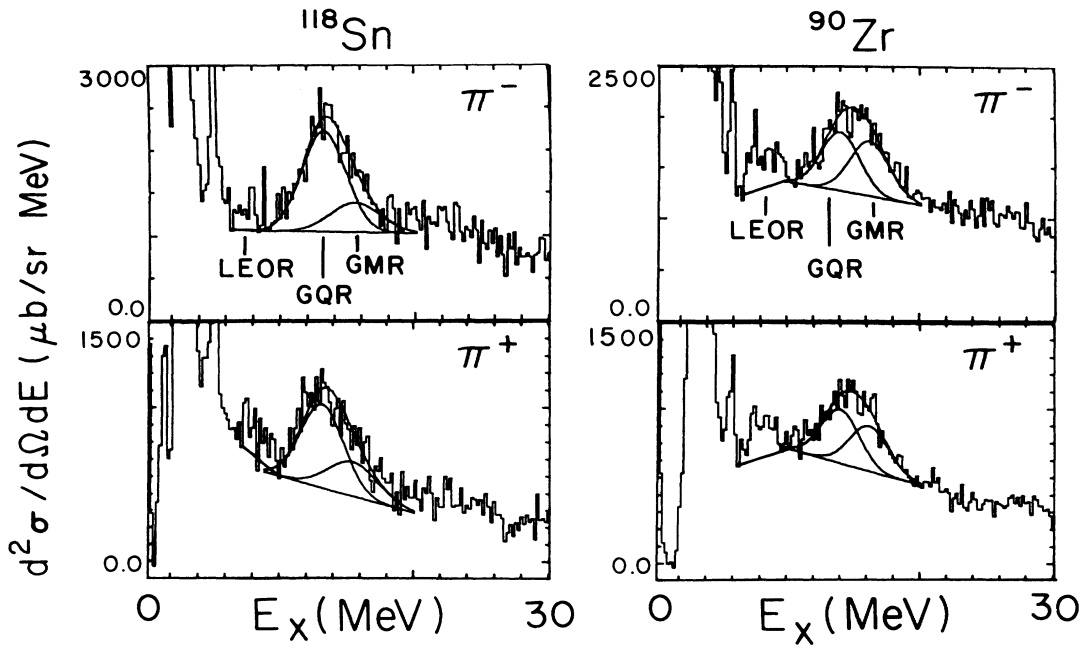

FIG. 2. The known LEOR, GQR, and GMR states of ^{90}Zr and ^{118}Sn near the $L=2$ maxima. The widths and centroids are those determined from alpha particle scattering, and the straight-line backgrounds are shown.

the subsequent range of counts as the uncertainty in the area. For the LEOR, the peak shape could not be represented by an analytic function, so for both targets all counts above a straight-line background were summed to determine the cross sections. The general features of the LEOR regions were found to be similar to those observed with other scattering probes.

The relative normalization of the data was made through an ion chamber (IC1) located downstream from the scattering targets. An ion chamber (BOT) viewing the carbon pion production target in the primary proton beam and a toroidal pickup loop around the primary beam were also used. All monitors gave consistent results, but the relative normalization was carried out using IC1.

The absolute normalization of the data was accomplished using elastic π^+-p scattering from a solid CH_2 target with the hydrogen measured by chemical means to an accuracy of 1.5%. Measurements were made at several different angles for this normalization and spectra were taken with a carbon target to aid in background subtraction. Pion-nucleon cross sections were obtained from the Arndt and Roper FP84 phase shifts.[5] The acceptance of the focal plane was also determined from π^+ scattering on carbon in the CH_2 targets at a range of spectrometer fields. This acceptance was slightly different for each target strip.

The overall uncertainty in the absolute values of the cross sections arose from two general sources. The statistical uncertainty was related to the extraction of the counts for a particular state in each target. The pion-beam monitoring, the wire-chamber efficiency, the pion survival fraction, the target thickness, and the choice of background were each estimated to contribute about 3% normalization uncertainty in the absolute cross section. A second source of uncertainty was related to the CH_2 normalization measurements where systematic uncertainties in the beam monitoring (3%), wire-chamber efficiency (3%), pion survival fraction (3%), CH_2 target thickness (1%), and counting statistics (π^- 3%, π^+ 1.5%) when combined in quadrature with uncertainties from the first source of normalization error yield about a 10% absolute normalization uncertainty for our π^+ or π^- data. The relative normalization between the π^+ and π^- data sets is known to about 8%.

Best values for the transition strengths $(\beta R)_+$ or $(\beta R)_-$ were found by a least-squares fit of the DWBA calculations to the entire π^+ or π^- angular distribution, unless a known contaminant was present. Uncertainties, however, were estimated by the extreme credible range of such fits. These uncertainties for the giant states were much larger than those obtained from the statistical results of the fitting routine, which did not include the inadequacy of the calculated shape. The parameters $(\beta R)_p$ and $(\beta R)_n$ were obtained by simultaneously reproducing the π^- and π^+ data using the best maximum cross section found by the fitting, since the shapes do not change. For simplicity, fractional uncertainties for $(\beta R)_p$ and $(\beta R)_n$ were set equal to those for $(\beta R)_+$ and $(\beta R)_-$, respectively. Deformations $(\beta R)_0$ and $(\beta R)_1$ were computed from $(\beta R)_p$ and $(\beta R)_1$.

B. Theoretical methods

The measured differential cross sections were compared to DWIA calculations performed with the code DWPIES,[6] without second-order effects. Both distortions and the π-nucleus interaction were determined from the π-nucleon amplitudes of Rowe, Salomon, and Landau.[7] An energy shift of $(35+0.3i)$ MeV as proposed in Ref. 8 was used in generating the distorted waves; the angular positions of the maxima in the DWIA predictions were not affected by this shift. Inclusion of this energy shift gave calculated π^- and π^+ inelastic cross sections smaller by roughly a factor of 0.8 for $L=0$, 2, and 3 than those computed without the shift. Larger normalizations, $(\beta R)^2$, thus result from comparing data to these calculations. Reanalysis of the 130-MeV data from Ref. 1 was done without an energy shift, since this shift has been determined only for resonance beam energies.[8]

Macroscopic transition densities were used in the DWIA analyses, with equal geometric parameters for neutrons and protons. Simple derivative transition densities $\rho_{\rm tr}(r)$ were used for low-lying transitions. However, it has been shown that the Tassie form is required[9] for a single transition exhausting the sum rule strength; hence Tassie transition densities were used for the giant resonance transitions of multipolarity greater than one. The DWIA code used[6] uses $\rho_{\rm tr}^T \sim (r/c)^{L-1}\rho'(r)$ for the Tassie transition density. For the nominal GMR transition at $80A^{-1/3}$ MeV, the volume-conserving transition density of model I of Ref. 10 was used. Since this transition density has a node near the nuclear surface, the details of the numerical integration can change the computed cross section. We used a radial step size of 0.05 fm and an outer cutoff of 10 fm, including 20 partial waves in the calculation. The data were normalized to the DWIA calculations by empirical collective parameters β or βR, which we take to represent the transition strengths.

The neutron and proton distributions used for the transition densities were also those that determine the optical potential. Woods-Saxon shapes with the same radius and diffuseness for neutrons and protons gave elastic scattering calculations in agreement with the data for both targets, as shown in Fig. 3. For ^{90}Zr we used radius $c=4.86$ fm, diffuseness $a=0.53$ fm and for ^{118}Sn we used $c=5.41$ fm, $a=0.517$ fm, as in our work at 130 MeV.[1] These ground-state geometrical parameters were determined from electron scattering analyses,[11] corrected for the proton finite size. Coulomb excitation was not included in our reaction calculations.

The π^- to π^+ comparisons may be made in three different ways. In the simplest view, the π^- and π^+ data may each be compared to hydrodynamic DWIA calculations, with N neutrons and Z protons deformed by a common βR and the parameters $(\beta R)_-$ and $(\beta R)_+$ thus obtained. Alternatively, the neutron amplitude $(\beta R)_{\rm n}$ and the proton amplitude $(\beta R)_{\rm p}$ were determined by simultaneously fitting both the π^- and π^+ data. The values of $(\beta R)_{\rm n}$ were mainly determined by the π^- cross sections and $(\beta R)_{\rm p}$ by the π^+ cross sections. Finally, the $(\beta R)_{\rm n}$ and $(\beta R)_{\rm p}$ were used to compute the isoscalar and isovector amplitudes, $(\beta R)_0$ and $(\beta R)_1$, for comparison to sum rules. For 3-3 dominance, these different parameters sets are related by:

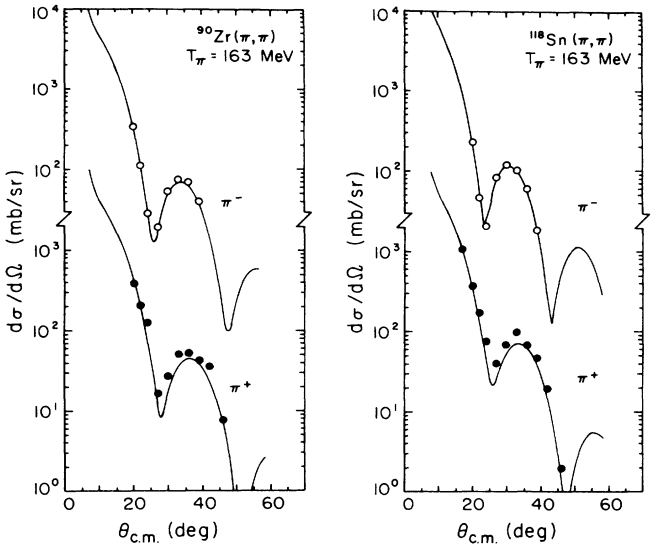

FIG. 3. Elastic scattering cross sections for ^{90}Zr and ^{118}Sn compared to optical model predictions (see the text). Equal geometric parameters were used for the neutron and proton distributions in each nucleus.

$$4A(\beta R)_0=(Z+3N)(\beta R)_-+(3Z+N)(\beta R)_+ , \quad (1a)$$

$$2(N-Z)(\beta R)_1=(Z+3N)(\beta R)_--(3Z+N)(\beta R)_+ , \quad (1b)$$

or

$$A(\beta R)_0=N(\beta R)_{\rm n}+Z(\beta R)_{\rm p} , \quad (2a)$$

$$(N-Z)(\beta R)_1=N(\beta R)_{\rm n}-Z(\beta R)_{\rm p} . \quad (2b)$$

If the hydrodynamic collective model and this 3-3 dominance were exact, we would have $(\beta R)_0=(\beta R)_1=(\beta R)_{\rm n}=(\beta R)_{\rm p}=(\beta R)_+=(\beta R)_-$. If the assumptions of the hydrodynamic model are not valid, for example if $(\beta R)_{\rm n}$ is not equal to $(\beta R)_{\rm p}$, the first symptom would be unequal values for $(\beta R)_-$ and $(\beta R)_+$. In those cases where this discrepancy was found, we varied $(\beta R)_{\rm p}$ and $(\beta R)_{\rm n}$ independently to fit simultaneously the π^+ and π^- cross sections. All $(\beta R)_0$ and $(\beta R)_1$ values were computed using the values of $(\beta R)_{\rm p}$ and $(\beta R)_{\rm n}$, as in Eq. (2). Our previous data[1] for ^{118}Sn at 130 MeV were refit by this prescription as well and compared to the sum rules of the present work. This method was also used for the GQR in ^{208}Pb.[2]

For the giant excitations, we also computed the energy-weighted transition strength for comparison to the energy-weighted sum rule (EWSR) strengths. For the isoscalar ($L\geq 2$) sum, for a single excitation described by a Tassie transition density at $\hbar\omega$ with deformation $(\beta R)_0$ exhausting the sum strength, this would be:[10]

$$\Sigma_0^T=(\beta R)_0^2=\frac{\hbar^2}{2mA}\frac{4\pi}{\hbar\omega}L\frac{c^{2L-2}}{\langle r^{2L-2}\rangle} . \quad (3)$$

The Tassie radial expansion parameter is the midpoint radius c in this expression, just as used in DWPIES.[6] For derivative transition densities, the sum rule differs due to different radial moments encountered, with

$$\Sigma_0^D=(\beta R)_0^2=\frac{\hbar^2}{2mA}\frac{4\pi}{\hbar\omega}\frac{L(2L+1)^2}{(L+2)^2}\frac{\langle r^{2L-2}\rangle}{\langle r^{L-1}\rangle^2} . \quad (4)$$

Ground-state distributions with the same geometrical parameters for neutrons and protons were used to evaluate radial moments for these sums. The $(\beta R)_0$ amplitudes obtained from the data for each form of the transition density are compared to Eq. (3) or Eq. (4) to form the isoscalar sum-rule fraction:

$$F_{\mathrm{SR},0}=(\beta R)_0^2/\Sigma_0 . \quad (5)$$

For a uniform distribution of radius R, Eqs. (3) and (4) become equal, giving a commonly used sum-rule strength,[12] as was used in our 130 MeV analysis.[1] The isoscalar $F_{\mathrm{SR},0}$ may be compared directly to results obtained for other probes, but there are no simple comparisons to sum rules using $(\beta R)_+$ and $(\beta R)_-$. For isovector transitions, the squared amplitude summed over all the isovector strength to satisfy the sum rule is[10]

$$\Sigma_1=(\beta R)_1^2=\Sigma_0 . \quad (6)$$

For the proton component of the vibration, we use

$$\Sigma_p=(\beta R)_p^2=A\Sigma_0/Z , \quad (7)$$

and for neutron components, we use

$$\Sigma_n=(\beta R)_n^2=A\Sigma_0/N . \quad (8)$$

Note that these expressions denoted by Σ are not the same as those using the same symbol in Ref. 2.

Our previous work at 130 MeV (Ref. 1) cited energy-weighted sum-rule (EWSR) fractions based on the derivative transition density, with uniform distributions to compute the isoscalar and isovector sum rules.

Although much of the isovector strength is expected to be concentrated into an isovector GQR at higher excitations, for a state of maximum symmetry between neutrons and protons (commonly called an isoscalar transition) in a target with a neutron excess, some isovector strength must also be present to prevent motion of the center of mass. The isovector strength anticipated in such an isoscalar mode is[13]

$$\Sigma_1'=\frac{N-Z}{A}\Sigma_0 . \quad (9)$$

For the giant monopole resonance (GMR), the isoscalar sum strength would be exhausted by[10]

$$[\beta(L=0)]^2=\frac{4\pi}{\hbar\omega}\frac{\hbar^2}{2mA}\frac{1}{\langle r^2\rangle} , \quad (10)$$

and the isovector by

$$[\beta(L=0)]_1^2=[\beta(L=0)]_0^2 .$$

We used the computed mean-square radii to evaluate this sum. As for the $L\geq 2$ case,

$$[\beta(L=0)]_p^2=\frac{A}{Z}[\beta(L=0)]_0^2$$

and

$$[\beta(L=0)]_n^2=\frac{A}{N}[\beta(L=0)]_0^2 .$$

To compute the monopole amplitude, we use βR with the half-radius of the matter distribution, c, for R as in Ref. 1.

The neutron and proton strengths may also be compared through their nuclear matrix elements M_n and M_p, as often used for analysis of low-lying collective states.[14,15] With equal shapes for neutron and proton densities, this gives $M_n/M_p=N\beta R_n/Z\beta R_p$, when βR_n and βR_p are obtained as described above. If the hydrodynamic picture is valid, that is $\beta R_n=\beta R_p$, then M_n/M_p becomes N/Z.

III. RESULTS FOR ^{118}Sn

A. Low-lying states

Data for the 1.23-MeV 2^+ state and the 2.31-MeV 3^- state of ^{118}Sn are shown for 163-MeV π^- and π^+ scattering in Fig. 4, compared to DWIA calculations. No better fits were obtained by varying $(\beta R)_p$ and $(\beta R)_n$ from the values predicted by Eqs. (1) and (2). The βR's are shown in Table I.

The three pairs of parameters used to present the various forms of βR are not independent, and all three were found to be equal in value, as would be expected from a

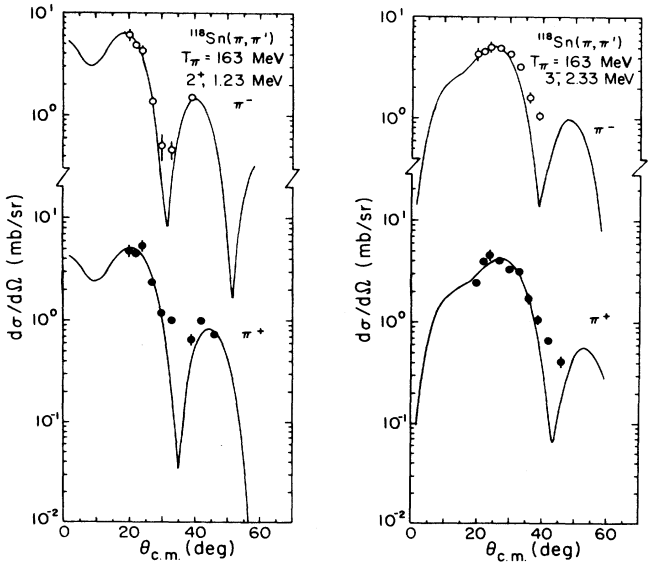

FIG. 4. Data for lowest 2^+ and 3^- states of ^{118}Sn compared to collective model DWIA predictions, normalized by the parameters βR_+ and βR_- listed in Table I.

TABLE I. Deformation lengths βR (in fm) for the 1.23-MeV 2^+ and 2.31-MeV 3^- states of ^{118}Sn are compared in three forms, using the present 163-MeV data. Results from earlier 130 MeV data are also shown. Comparisons to isoscalar and electromagnetic results are also listed. Derivative form factors are used, with an energy shift for the 163 MeV results. In this table, and in the following presentations, normalization uncertainties are not included. See Sec. II A.

	2^+		3^-	
	163 MeV	130 MeV[a]	163 MeV	130 MeV[a]
$(\beta R)_+$	0.82±0.06	0.84±0.08	1.09±0.08	0.99±0.09
$(\beta R)_-$	0.80±0.06	0.87±0.08	1.01±0.07	1.01±0.09
$(\beta R)_0$	0.81±0.04	0.86±0.08	1.05±0.05	1.00±0.09
$(\beta R)_1$	0.68±0.22	1.05±0.64	0.53±0.16	1.13±0.66
$(\beta R)_p$	0.83±0.10	0.82±0.08	1.14±0.14	0.98±0.09
$(\beta R)_n$	0.79±0.09	0.88±0.08	0.98±0.10	1.02±0.09
$(\beta R)_0$ (α,α')[b]	0.65		0.73	
$(\beta R)_p$ (em)[c]	0.64		0.92	
$(\beta R)_0$[d]	0.69±0.02			
$(\beta R)_1$[d]	1.47±0.28			

[a]Reference 1.
[b]Reference 16.
[c]Reference 18.
[d]Reference 17.

hydrodynamic weighting using the relations of Eqs. (1) or (2). Table I also compares the current results to our earlier experiment (Ref. 1). Except for the isovector $(\beta R)_1$'s, the two experiments are in excellent agreement. Due to sensitive cancellations in comparing $(\beta R)_+$ and $(\beta R)_-$, the isovector parameters become unreliable, as noted by their errors. In essence, this is due to the subtraction of experimental results to evaluate the βR_1 parameter. This is clearly a somewhat inaccurate process.

A comparison to other probes is also made in Table I. The isoscalar $(\beta R)_0$ results of 0.81 fm and 1.05 fm for the 2^+ and 3^- states are appreciably greater than those determined by alpha-particle scattering, 0.65 fm and 0.73 fm, respectively,[16] or by neutron and proton scattering to the first 2^+ state,[17] 0.69 fm. The $(\beta R)_p$ values of 0.83 and 1.14 fm are also greater than those determined by electron scattering, 0.64 and 0.92 fm.[18] Overall, for both states, the pion βR values are greater by a factor of about 1.3 than those measured with other probes. We note that if we had not used the energy shift in our DWIA calculations, our $(\beta R)^2$ values would be smaller by about a factor of 0.8, which would give better agreement with values obtained in the electron and alpha particle scattering analyses.

The 2^+ data from different probes may also be compared by a deformation parameter versus interaction strength plot as suggested in Ref. 14. This was done in Ref. 1, and the current data are in good agreement with the data presented there. The ratio of M_n/M_p from Table II can be compared to the results of other probes and theoretical values as displayed in Ref. 14. We find in both comparisons that our data for the first 2^+ state are in agreement with $M_n/M_p = N/Z = 1.36$, and therefore in disagreement with conclusions obtained from comparisons of several probes and with the theory of Ref. 19, which predicts M_n/M_p in the range of 1.6 to 1.7.

B. Giant resonances

Figure 5 shows the angular distributions for the giant resonances in ^{118}Sn along with DWIA calculations. The solid curves are normalized to the data by a least-squares fit of the parameters $(\beta R)_+$ and $(\beta R)_-$ independently to the π^+ and π^- data, respectively. The dashed curves in Fig. 5 result from a simultaneous fit of the parameters $(\beta R)_p$ and $(\beta R)_n$ to both the π^+ and π^- data. Somewhat less sharp diffractive structure is found by this method. The βR values are listed in Table III. As was noted before,[1] there is a striking excess of π^- over π^+ strength for the GQR. At 130 MeV, the ratio of GQR squared amplitudes $(\beta R)^2$ for π^- over π^+ was 1.51 ±0.20, while this has increased to 2.3±0.4 at 163 MeV. The ratio of GQR cross sections at maximum is 1.9±0.4 at 130 MeV, but 2.3±0.25 at 163 MeV.

When the βR values were combined to form isoscalar or isovector strengths, we obtained the deformation lengths listed in Table III. The isoscalar strength to the ^{118}Sn GQR exhausts 56±9 % of the isoscalar sum rule at 163 MeV, only a bit less than found for alpha-particle scattering, as in Table III. A more extensive comparison of the results from several scattering probes is found in Ref. 1. When cast in terms of an isovector strength, the GQR of ^{118}Sn is found to exhaust (460±500 %) of the isovector sum rule Σ_1 of Eq. (6). The isovector sum strength from the present analysis of the data at 130 MeV (Ref. 1) is (260±100)% of the result computed from Eq. (6).

The $L=0$ fits at 163 MeV to the nominal GMR state at 15.5 MeV are shown in Fig. 5, with β_+ and β_- equal to 0.067 and 0.087, respectively; these are listed in Table III as βR. These calculated angular distributions do not disagree with the observed shapes, but the fit to the π^+ magnitude is not good. It has been suggested that the dipole state, at the same excitation as the GMR, is respon-

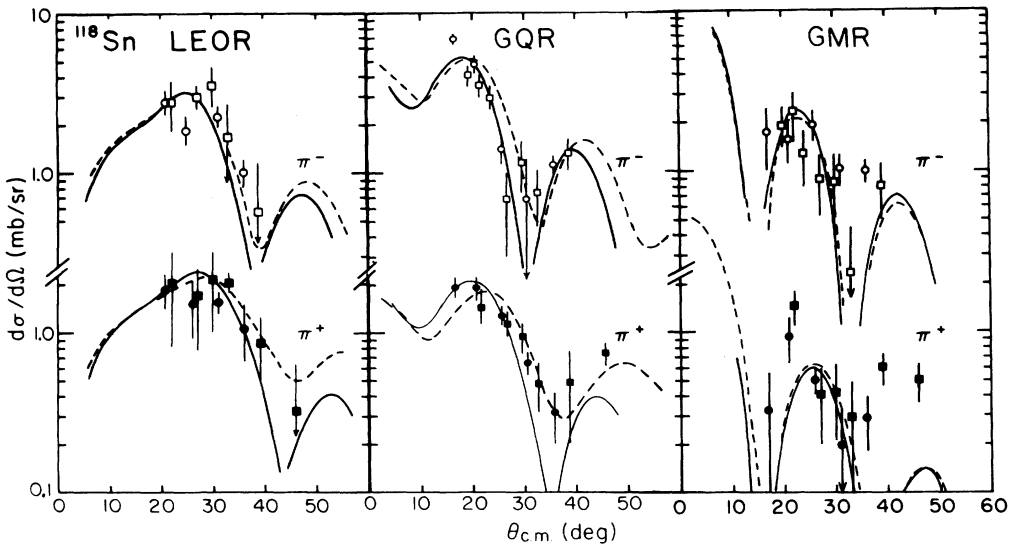

FIG. 5. Data for the LEOR, GQR, and GMR in ^{118}Sn compared to DWIA predictions using the Tassie or monopole form factors, normalized to βR_+ and βR_- as listed in Table III as the solid curves. Dashed curves show the fits to βR_p and βR_n. Circle or square data points are for cross sections obtained with two settings of the spectrometer magnetic field, as detailed in the text.

TABLE II. Matrix elements for the transitions in this work are listed in fm^{2L}, and $B(CL)\uparrow$ values are listed in e^2fm^{2L}. Derivative transition densities are used for the low states and the Tassie forms for giant states. These alternative ways to present our results are compared to the work of others. For ^{118}Sn, the pion results at 163 and 130 MeV have been averaged. A collective transition density has been used for all analyses to yield these results.

^{90}Zr	2_1^+	3_1^-	LEOR	GQR
M_n	32	302	157	33
M_p	34	348	138	22
M_0	66	650	295	55
$B(CL)\uparrow$	1160	1.21×10^5	1.90×10^4	490
$B(CL)\uparrow$	674[b]	1.08×10^5[c]		990±300[d]
M_n/M_p	0.947	0.868	1.14	1.48
M_n/M_p	1.12±0.04[a]	1.06±0.05[a]		
N/Z	1.25			
^{118}Sn				
M_n	80	575	352	62
M_p	58	448	272	26
M_0	138	1023	624	87
$B(CL)\uparrow$	3350	2.02×10^5	7.41×10^4	664
$B(CL)\uparrow$	2000±30[a]	1.1±0.2×10^5[a]		
	1990±60[e]			
M_n/M_p	1.38	1.29	1.29	2.38
M_n/M_p	1.87±0.03[a]	1.84±0.03[a]		
	1.72[d]			
N/Z	1.36			

[a]Reference 28, for ^{120}Sn.
[b]Reference 25.
[c]Reference 30.
[d]Reference 37.
[e]Reference 41, for ^{118}Sn.

TABLE III. Deformation lengths βR and $F_{SR}=(\beta R)^2/\Sigma$ are listed for the giant states of ^{118}Sn at two pion-beam energies; both data sets are analyzed by the same methods using the Tassie transition densities. An energy shift was used at 163 MeV but not at 130 MeV. A sample of comparisons to the results from other reaction probes is also made below. Normalization uncertainties are not included.

	LEOR		GQR		GMR	
E_x (MeV)	7.0		13.2		15.5	
Γ (MeV)			3.8		4.4	
T_π (MeV)	163 MeV	130 MeV[a]	163 MeV	130 MeV[a]	163 MeV	130 MeV[a]
$(\beta R)_+$ (fm)	0.47±0.04	0.47±0.02	0.40±0.05	0.39±0.06	$0.35^{+0.18}_{-0.06}$	0.40±0.08
$(\beta R)_-$ (fm)	0.47±0.04	0.45±0.02	0.61±0.07	0.48±0.03	0.58±0.07	0.57±0.03
$(\beta R)_p$ (fm)	0.47±0.04	0.49±0.01	0.34±0.05	0.32±0.06	$0.42^{+0.20}_{-0.07}$	0.27±0.05
$(\beta R)_n$ (fm)	0.47±0.04	0.44±0.02	0.64±0.07	0.52±0.04	0.65±0.07	0.66±0.04
$F_{SR,p}$ (%)	6.9±1.2	7.4±0.3	10.6±3.5	9.4±3	32^{+36}_{-12}	15±2
$F_{SR,n}$ (%)	9.4±1.6	8.2±0.8	51±10	34±5	102±24	128±13
$(\beta R)_0$ (fm)	0.47±0.03	0.46±0.03	0.51±0.05	0.44±0.05	$0.56^{+0.13}_{-0.07}$	0.44±0.04
$(\beta R)_1$ (fm)	0.48±0.19	0.30±0.13	1.46±0.84	1.09±0.7	$1.3^{+1.8}_{-1.0}$	1.42±0.84
$F_{SR,0}$ (%)	16±2	16±2	56±9	42±4	130^{+65}_{-35}	124±10
$F_{SR,1}$ (%)	17±13	6.6±5	460±540	258±100	700^{+2000}_{-650}	1570±700
$F_{SR,0}$ (α,α')	20[b]		60[c]		150[c]	
$F_{SR,0}$ (α,α')[f]			70±15		100±20	
$F_{SR,p}$			65			
F_{SR} (p,p')[e]			37±7		18±34	

[a]Reference 1.
[b]Reference 21.
[c]Reference 4.
[d]Reference 22, for ^{116}Sn.
[e]Reference 23, for ^{120}Sn.
[f]Reference 16, for ^{120}Sn.

sible for alpha scattering to this peak.[20] Only a monopole analysis is reported here. When β_n and β_p were varied to fit these data simultaneously, as shown by the dashed curves, values of 0.108 and 0.071 are found, respectively. These exhaust (130^{+65}_{-35}%) of the monopole isoscalar EWSR and (700^{+2000}_{-650}%) of that for the isovector EWSR. At 130 MeV, these fractions were (124±10)% isoscalar and (1570±700)% isovector, when reanalyzed using the present scheme. These isoscalar results are in adequate agreement, essentially exhausting the isoscalar EWSR if this is a monopole excitation. The discrepancy between the isovector results at the two energies may be due to the great sensitivity in comparing in this fashion π^- and π^+ data, and to the quality of the data. It should be noted that an energy shift was used at 163 MeV and not at 130 MeV.

These enhanced ratios of π^- over π^+ cross sections for the GQR and GMR are in contrast to the results for the LEOR, which is a broad distribution of strength from 4.6 to 8.4 MeV in excitation.[21] The angular distributions we measured at 163 MeV are shown in Fig. 5, together with DWIA calculations. The π^-/π^+ cross-section ratio at the maximum of the differential cross section is 1.28±0.18, compared to 2.3±0.25 for the GQR. The values of βR are listed in Table III, derived in just the fashion used above for the GQR and GMR. The results at 130 MeV, when reanalyzed in this same fashion, are also shown. At both energies, all pairs of βR are roughly equal, implying a hydrodynamic nuclear transition. The isoscalar $F_{SR,0}$ strength of 16% is a bit less than the 20% found by alpha particle scattering.[21]

In Ref. 1 the analysis of the 130 MeV data for ^{118}Sn used a derivative transition density rather than the Tassie form used here for the LEOR. The greater surface weighting of the present DWIA predictions (especially for $L=3$) requires smaller transition strengths to match the data and smaller amplitudes were thus obtained. This accounts for the discrepancy between the present results in Table III and those of Ref. 1. In Table II the matrix elements and reduced transition rates of the LEOR in ^{118}Sn are also listed.

Since the LEOR is the $1\hbar\omega$ component of the octupole vibration mode and therefore is expected to be at only one third the excitation energy of the $3\hbar\omega$ high energy octupole resonance (HEOR), the EWSR strength is expected to be but one fourth of the total. (See Ref. 13, p. 556.) From Table III, we see that even a smaller value than this is found for ^{118}Sn, using the Tassie transition density. If a simple derivative form is used for the DWIA predictions, the isoscalar EWSR fraction (F_{SR}) exhausted for $L=3$ increases to 19%, which also nearly agrees with this smaller expectation.

IV. RESULTS FOR ^{90}Zr

A. Low-lying transitions

Angular distributions for the 2^+ state of ^{90}Zr at 2.18 MeV and for the 3^- state at 2.75 MeV are shown in Fig. 6. The solid curve for the 2^+ state shows the DWIA cal-

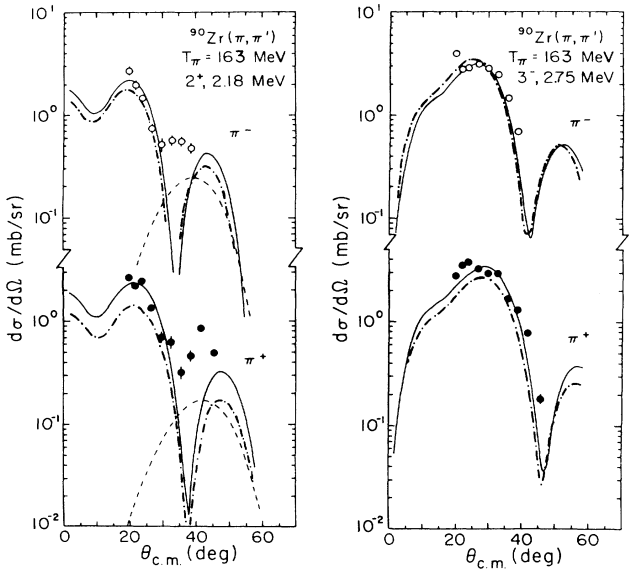

FIG. 6. Data for lowest 2^+ and 3^- states of ^{90}Zr compared to collective model DWIA predictions as the solid curves, normalized by βR_+ and βR_-. The dashed curve shows the cross section predicted for the 2.32-MeV 5^- state, not resolved from the 2.18-MeV 2^+ state. The dot-dash curves show the DWIA predictions using proton transition densities determined from electron scattering (Ref. 34) and a neutron transition density taken to be N/Z times these proton transition densities.

culation with a derivative transition density with values of $(\beta R)_+ = 0.62$ fm and $(\beta R)_- = 0.53$ fm. A significant π^+ or proton-like enhancement is indicated.

At angles beyond 30 deg the data fail to show the expected diffraction minimum. Since the 5^- state at 2.32 MeV could not be resolved from the 2^+ state, some $L=5$ contribution is expected. In Fig. 6 the dashed curves show the DWIA prediction for $L=5$ using a value of $\beta R = 0.38$ fm, as observed in inelastic alpha-particle scattering.[24] It is seen that this transition does not contribute to the region of the first 2^+ maximum where we obtained our normalizations.

We also varied $(\beta R)_p$ and $(\beta R)_n$ separately for simultaneous agreement with both π^+ and π^- data. These are listed in Table IV, and again show a departure from the hydrodynamic expectation of equal βR amplitudes. These $(\beta R)_p$ and $(\beta R)_n$ results are combined to give the indicated isoscalar and isovector deformation lengths in Table IV.

The negative sign for $(\beta R)_1$ for the 2^+ state indicates a proton-like amplitude, and although the uncertainty is not small, a strong deviation from the hydrodynamic prediction $(\beta R)_0 = (\beta R)_1$ is noted. The isoscalar amplitude $(\beta R)_0$ for this 2^+ is slightly above the results from other probes (listed in Table IV), an effect also noted for the lowest 2^+ state of ^{118}Sn.

A proton amplitude $(\beta R)_p$ for this 2^+ transition may be inferred from the "combined" electromagnetic result of Singhal *et al.*,[25] with $(\beta R)_p$ equal to 0.50 ± 0.02 fm. This is lower than that from the present work. Since a collective derivative transition density was used for all of these analyses, these inconsistencies may reflect the inadequacy of this model.

By comparing the isoscalar nuclear and the Coulomb excitation amplitudes for scattering 35 MeV alpha particles to the lowest 2^+ state of ^{90}Zr, Lahanas *et al.*[26] obtained a sharp chi-squared minimum at 1.45 for the ratio β_p/β_0, or 1.15 for the ratio of deformation lengths $(\beta R)_p/(\beta R)_0$, where R_0 is the optical model radius and R_p is c. This ratio is proton-like, and in good agreement with the pion work, where we obtain $(\beta R)_p/(\beta R)_0 = 1.16 \pm 0.12$.

For the 2.75-MeV 3^- transition the values of $(\beta R)_p$ and

TABLE IV. Deformation lengths βR (in fm) for the 2.186-MeV 2^+ and 2.748-MeV 3^- states of ^{90}Zr from the 163 MeV data are compared in three forms. These parameters were obtained as described in the text. These results are plotted by their probe dependence in Fig. 7.

	2^+	3^-
$(\beta R)_+$	0.62±0.04	1.10±0.10
$(\beta R)_-$	0.53±0.04	0.92±0.06
$(\beta R)_p$	0.66±0.05	1.21±0.12
$(\beta R)_n$	0.50±0.05	0.84±0.06
$(\beta R)_0$	0.57±0.04	1.01±0.06
$(\beta R)_1$	−0.14±0.08	0.61±0.33
$(\beta R)_0$ ($\alpha\alpha'$, 96 MeV)[a]	0.42±0.06	0.77±0.12
$(\beta R)_0$ ($\alpha\alpha'$, 31 MeV)[b]	0.38	0.64
$(\beta R)_0$ (pp', 800 MeV)[c,d]	0.465±0.008	0.89±0.02
	0.46	0.75
$(\beta R)_p$	0.504±0.021[f]	1.14±0.11[e]
$(\beta R)_0$ (pp')[g] and (nn')[g]	0.42±0.02	
$(\beta R)_1$ (pp')[g] and (nn')[g]	−0.30±0.09	
βR (pp', 65 MeV)[h]	0.355	0.79

[a]Reference 27.
[b]Reference 24.
[c]Reference 28.
[d]Reference 29.
[e]Reference 30.
[f]Reference 25.
[g]Reference 31.
[h]Reference 32.

$(\beta R)_n$ that yield the best simultaneous agreement with the π^+ and π^- data show some proton-like enhancement. This is noted as a negative value of $(\beta R)_1$, as was also obtained for the 2^+ transition. The isoscalar amplitude $(\beta R)_0$ exceeds the values from proton or alpha-particle scattering, as seen in Table IV. The proton amplitude is in agreement with that from electron scattering.[30]

The deformation lengths βR obtained with different probes are compared in Fig. 7. The values of $(\beta R)_+$ and $(\beta R)_-$ as listed in Table IV are plotted along with theoretical predictions from Ref. 19. For the 2^+ state, the pion data show a definite proton enhancement by the downward slope, but with a magnitude somewhat higher than obtained with other probes.

The ratios of $(\beta R)_n/(\beta R)_p$ from the present analysis are 0.76 ± 0.06 and 0.69 ± 0.07 for the 2_1^+ and 3_1^- transitions. These are in fair agreement with the values of 0.90 and 0.85 found by comparison of 800 MeV proton scattering and electromagnetic transitions to these same states,[28] assuming the same collective transition density as used in the present case. These results may be compared to the ratio of effective charges for neutrons and protons for a shell-model treatment of the 2_1^+ transition, where e_n/e_p is computed to be 0.83 or 0.80 in two forms of the calculations.[33] For the 2^+ state, the M_n/M_p ratio (0.95 ± 0.08) is in good agreement with "OPSM" theory of Ref. 19, which predicts a ratio of 0.97,[14] and with this ratio measured using other probe combinations.[14] These are summarized in Ref. 15.

In addition to these collective analyses, we may make a direct comparison for ^{90}Zr to the proton transition densities determined by a Fourier-Bessel analysis of electron-scattering form factors. These are available for the 2.18 MeV 2^+ state and the 2.75 MeV 3^- state.[34] Radial transition densities for the neutrons were taken as N/Z times those for protons, as expected for a collective transition. These transition densities were used in the code DWPIES, with distortions treated as for the other computations. The resulting absolute predictions are compared to the data in Fig. 6 as the dot-dashed curves.

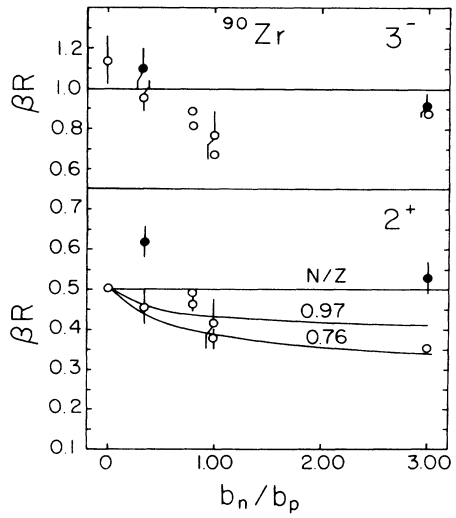

FIG. 7. Deformation parameters for different probes plotted versus the ratio of probe-nucleon couplings. The closed circles are from this work and the open circles are for other probes, all tabulated in Table IV. The lines labeled N/Z, 0.97 and 0.76 are for $M_n/M_p=N/Z$, 0.97 and 0.76, respectively. The latter values are calculated in Ref. 19.

For the 2.19 MeV 2^+ state, those predictions are decidely low, especially for the π^+ data. No reasonable changes to the neutron distribution have enough effect on the π^+ prediction to bring agreement. Better agreement is found for the π^+ data to the 3^- state. While a small increase of the neutron transition density beyond N/Z times the proton transition density would help the π^- fit to the 2^+ data, and a decrease to less than N/Z would improve the π^- agreement with the 3^- data, these reasonable changes could have only a weak effect on the π^+ predictions, which are in great disagreement with the data.

The failure of these well-determined transition densities to yield the correct π^+ cross sections is a major disagreement, indicating serious problems for the 2^+ state in particular. We point out, however, that the electron and pion beams probe different radial regions of the transition density, and the electron-scattering results may be a poor guide to the region of large radius.

To check the consistency of this type of comparison we also used the Fourier-Bessel densities from electron scattering[35] to compute pion inelastic scattering for well-known collective transitions to the first 2^+ state in ^{58}Ni and the first 3^- state in ^{208}Pb. For both π^+ and π^-, for both targets, very good agreement was found with pion scattering data at 162 MeV.[36] Only for the less collective transitions in ^{90}Zr is disagreement found between the two probes.

B. Giant resonances

Angular distributions for the giant resonances of ^{90}Zr are compared to DWIA calculations with Tassie transition densities in Fig. 8. The solid curves are based on fitting $(\beta R)_+$ and $(\beta R)_-$ while the dashed curves are from simultaneously fitting $(\beta R)_p$ and $(\beta R)_n$. The shapes of these two curves are more similar than they were for ^{118}Sn. The values of the extracted (βR) parameters are listed in Table V along with the sum rule fractions. At the peak of the angular distributions the ratio of π^- to π^+ cross sections for the GQR is 1.60 ± 0.21, and the ratio $(\beta R_-)^2/(\beta R_+)^2$ is 1.35 ± 0.17. The transition to the GQR exhausts $(31\pm3)\%$ of the isoscalar EWSR for ^{90}Zr, only about half that found in alpha particle scattering (See Table V). When combined to form the proton sum-rule fraction, $F_{SR,p}$ the present result of $(11\pm2)\%$ is much less than the strength found in electron scattering,[37] $(56\pm17\%)$.

For ^{90}Zr we may also compare our GQR results to earlier π^+ data. At the same beam energy, on a ^{89}Y target, cross sections very near to our π^+ results are found.[38] However, the fraction of the EWSR reported in that work is twice that inferred from our analysis, being 50% instead of $(31\pm3\%)$. At a higher beam energy (226 MeV) on ^{90}Zr, a similar analysis yielded an EWSR fraction of 45%.[39] This disparity indicates a disquieting disagree-

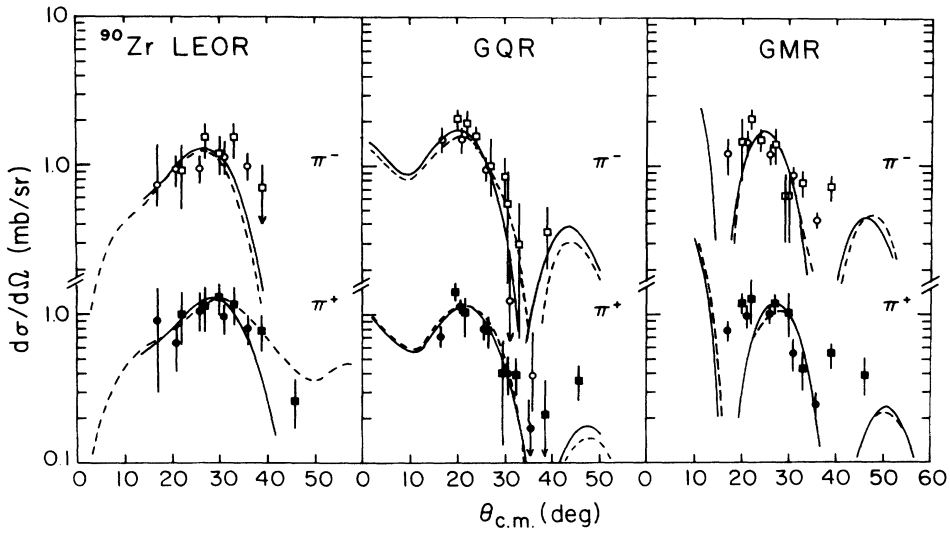

FIG. 8. Cross sections for the giant resonances in ^{90}Zr for the low (circles) and high (squares) spectrometer field settings. The solid lines are DWIA calculations, using Tassie transition densities for the LEOR and GQR, normalized to the π^+ and π^- data individually. The dashed curves are for the best fits to $(\beta R)_p$ and $(\beta R)_n$.

TABLE V. Deformation lengths and $F_{SR}=(\beta R)^2/\Sigma$ for the giant states of ^{90}Zr are listed. Below are comparisons to results using other reaction probes. Tassie transition densities and energy shifts are used for these analyses.

	LEOR	GQR	GMR
E_x (MeV)	7.25[h]	14.0[b]	16.2[b]
Γ (MeV)	1.87	3.4	3.5
$(\beta R)_+$ (fm)	0.34±0.03	0.31±0.03	0.57±0.07
$(\beta R)_-$ (fm)	0.31±0.03	0.36±0.03	0.60±0.05
$(\beta R)_p$ (fm)	0.34±0.03	0.37±0.03	0.63±0.07
$(\beta R)_n$ (fm)	0.31±0.03	0.44±0.03	0.60±0.05
$F_{SR,p}$ (%)	3.5±0.6	11.4±1.8	75±17
$F_{SR,n}$ (%)	3.6±0.7	20.0±3	85±14
$(\beta R)_0$ (fm)	0.33±0.02	0.41±0.02	0.61±0.04
$(\beta R)_1$ (fm)	0.19±0.11	0.72±0.34	0.48±0.29
$F_{SR,0}$ (%)	7.0±0.9	31±3	160±20
$F_{SR,1}$ (%)	2.4±2.8	95±68	98±82
$F_{SR,0}$ (800 MeV pp')[a]	20^{+9}_{-4}		
$F_{SR,0}$ ($\alpha\alpha'$)	20±5[i]	66±17[b]	90±20
$F_{SR,0}$ ($\alpha\alpha'$)[c]		65±13	80±20
$F_{SR,p}$ (ee')[d]		56±17	
$F_{SR,+}$ (^{89}Y, 163 MeV)[e]		50	20
$F_{SR,+}$ (^{90}Zr, 226 MeV)[f]		45	
F_{SR} (pp') (^{92}Zr)[g]		43±6	27±12
F_{SR} (pp')[h]	11.2		

[a]Reference 40.
[b]Reference 4.
[c]Reference 16.
[d]Reference 37.
[e]Reference 38, unknown transition density for GQR.
[f]Reference 39, unknown transition density for GQR.
[g]Reference 23.
[h]Reference 32.
[i]Reference 21.

ment in the DWIA predictions or in the usage of sum rules. The earlier work did not include π^- scattering, so no consistent isoscalar sum-rule analysis is possible.

The angular distribution for the 16.2 MeV peak, commonly interpreted[27] as the GMR of ^{90}Zr, is shown in Fig. 8. DWIA calculations with the volume-conserving transition density yield the curves shown for both pion charge states. The $(\beta R)_+$ and $(\beta R)_-$ are listed in Table V. When $(\beta R)_p$ and $(\beta R)_n$ are varied to fit both sets of data simultaneously, the amplitudes are 0.63 ± 0.07 fm and 0.60 ± 0.05 fm, respectively, and no excess of the neutron strength is found. When recast into isospin amplitudes $(\beta R)_0$ and $(\beta R)_1$, an excess of the isoscalar strength over the isovector strength is found. This isoscalar strength exhausts $(160\pm20)\%$ of the isoscalar monopole EWSR. This is much as found for ^{118}Sn. The isovector EWSR strength in this region, $F_{SR,1}$, is $(98\pm80)\%$.

The LEOR of ^{90}Zr was analyzed with a straight-line background as used for ^{118}Sn, over the region from 6.4 to 10 MeV in excitation. This is consistent with the regions reported in Refs. 21 and 32. No peak fit was made, and only counts above the background were summed. The angular distributions in Fig. 8 show a clear $L=3$ signature. Separate adjustment of $(\beta R)_n$ and $(\beta R)_p$ gave the results in Table V, showing only an insignificant neutron enhancement. Only small fractions of the EWSR are exhausted, even less than found in proton scattering studies[32,40] on ^{90}Zr.

V. DISCUSSION

A. Low-lying states

The low-lying states were studied to provide a test of our understanding of the reaction mechanism and nuclear structure in a region well-studied theoretically and experimentally. The elastic data are well represented by calculations using densities with equal neutron and proton radii and an impulse-approximation π-nucleus reaction mechanism including an energy shift. Although the elastic calculations would be improved by using the second-order corrections of Ref. 8 we elected to use only the energy-shift correction in the distorted waves for our inelastic calculations, to enable comparison to a similar elastic calculation.

For the 2_1^+ state in ^{118}Sn, we observe an M_n/M_p ratio (or ratios of the deformation lengths βR) considerably closer to the hydrodynamic (N/Z) value than observed with other probes or predicted theoretically by the core polarization model.[15,19] The pion data for the 3_1^- state were also consistent with N/Z weighting, but again M_n/M_p ratio determinations with other probes did not yield this simple result. Averaging over the two incident energies, we obtain $(\beta R)_0=(\beta R)_p=0.83\pm0.20$ for the 2^+ state and 1.04 ± 0.04 for the 3^- state. These exceed the (α,α') $(\beta R)_0$ and electromagnetic $(\beta R)_p$ results for this 2^+ state by a factor of 1.29, and the well-determined $(\beta R)_0$ for the 3^- state by a factor of 1.42 (see Table I).

For ^{90}Zr, our M_n/M_p ratio for the 2_1^+ state is consistent with the proton-like enhancement predicted by the core polarization model (which gives 0.97) (Ref. 14) and with other probes,[15] although our individual deformation lengths are somewhat larger than observed by others. Calculations using a "model-independent" form for the proton transition density from electron scattering underestimate the data, especially the π^+ data which should be the best determined by this comparison. This discrepancy is also evident in the $B(C2)$ values listed in Table II.

For the 3_1^- state of ^{90}Zr, our ratio M_n/M_p is in fair agreement with other results, as shown in Table II, and is less than N/Z, indicating a proton-like enhancement. Our $B(C3)$ is in good agreement with electron scattering and the model-independent comparison to the electron scattering transition density is quite good.

Inelastic π^-/π^+ scattering comparisons should provide the most consistent results for neutron/proton contributions in inelastic scattering. Except for the 2_1^+ level of ^{90}Zr, the M_n/M_p ratios we measured are less than observed by others, and the $(\beta R)_p$ values greater. The 2_1^+ level of ^{90}Zr is anomalous, and perhaps its weakly-collective structure is not properly treated in our simple analysis. Except for this transition, our data my be interpreted as consistent with either an enhanced proton-like amplitude or a reduced isovector transition strength. The latter may reflect uncertainty in the π-nucleus reaction mechanism but is in the opposite direction from calculations based on the delta-hole model[42] or an analysis of elastic scattering and single-charge exchange,[9] which yield an enhanced isovector strength. Another complication may arise from other resonances, although it has been pointed out that $T=\frac{1}{2}N^*$ virtual excitations will be small for the electric transitions considered in the present work.[43]

B. Giant resonances

The meaningful sum-rule comparisons involve the isoscalar, isovector, neutron, or proton sum rules discussed in Sec. II B. We note that there is little consistency in reporting sum-rule fractions from experimental results. Electron-scattering results are usually derived using a Tassie transition density, while alpha-scattering results are usually based on the derivative-collective form. Our present analysis used the Tassie form for $L\geq2$. Use of a derivative transition density would yield sum-rule fractions about 10% to 20% larger.

The isoscalar sum rule fractions we observed for the giant resonances in ^{118}Sn agree quite well with those obtained from alpha scattering. The agreement would be even better if we had also used a derivative transition density. For ^{90}Zr, our isoscalar sum-rule fractions for the LEOR and GQR are considerably less than observed by others. The proton sum-rule fractions we observed for the GQR are also considerably less than inferred from electron scattering.

The most striking result of this experiment is the large π^-/π^+ cross section ratio for the GQR and GMR. This is most easily seen in the M_n/M_p ratios, Table II, which are greater than N/Z for both ^{90}Zr and ^{118}Sn. This behavior is qualitatively different for the LEOR, where the M_n/M_p ratio is close to, or even slightly less than N/Z. In this respect, the LEOR shows the same features as observed for the low-lying states in both ^{90}Zr and ^{118}Sn.

The mass dependence of the ratio $d\sigma(\pi^-)/d\sigma(\pi^+)$ for the GQR at the peak of the angular distribution is shown in Fig. 10. Also shown is the calculated $d\sigma(\pi^-)/d\sigma(\pi^+)$ for a Tassie transition density assuming the hydrodynamic model, $M_n/M_p=N/Z$. The GQR for all targets with $N>Z$ seems to exhibit a neutron-like (π^-) enhancement, and we observe a systematic increase in the observed ratio over the N/Z ratio with increasing A.

There are two possible classes of explanations for this enhancement. The first is due to nuclear structure. Since the GQR is an unbound state, the strong π^- enhancement may be due to features of the transition density at the nuclear surface. A distinct difference between the GQR/GMR region and the LEOR is that the GQR and GMR are above the neutron binding energy while the LEOR is bound. Proton binding energies are less important in heavy nuclei due to the Coulomb barriers. The neutron-unbound transitions uniformly show a neutron-like (π^-) response in pion scattering, but this is not seen for the bound states, even the broad LEOR. Calculations in a single-particle model[44] show that this is just the effect expected for scattering to unbound states.

Auerbach *et al.*[45] have made continuum random phase approximation (RPA) calculations of the $d\sigma(\pi^-)/d\sigma(\pi^+)$ ratio. These are indicated in Fig. 10. The calculations include coupling to the continuum, but although they predict an increased $d\sigma(\pi^-)/d\sigma(\pi^+)$ ratio, the results still fall systematically below the data. For ^{208}Pb, an alternative RPA calculation[46] yields a similar result.

Reaction mechanism effects could also produce an increased ratio. Calculations based on the delta-hole model[42] and empirical studies of a second-order optical model[8] both indicate an enhancement of the isovector piece of the π-nucleon interaction in the nuclear medium. However calculation of the cross section ratio using the RPA transition densities and the isovector enhancement of Ref. 42 in the distorted waves indicates only a 6% increase in the predicted ratio.[45] Our data indicate that about a factor of 2 enhancement in the isovector part of the transition operator is needed to reproduce the ratios for the giant states. This is far greater than needed for elastic scattering in Ref. 8. Thus, it seems unlikely that reaction mechanism effects alone could account for the observed cross section ratio. Moreover, any modifications to the reaction mechanism would require an enhancement of the isovector amplitude to account for the giant resonance ratio, while the interpretation of the low-lying states would, if anything, imply the need for a diminished isovector amplitude.

A further clue to the origin of these asymmetries is found when we compare the π^- to the π^+ cross section to the continuum between 20 and 24 MeV of excitation, well above the standard giant states. These data are shown in Fig. 9. A π^-/π^+ cross section ratio of 1.5 is observed for ^{90}Zr and 2.3 for ^{118}Sn. These are to be compared to ratios of 1.48±0.19 and 2.10±0.23 for the GQR cross sections for these targets, at their maxima.

The pion inelastic continuum has recently also been studied by several other authors.[47–49] The only π^-/π^+ ratios for inelastic scattering in heavier nuclei are given by McKeown *et al.*,[48] who report angle- and energy-integrated yields for the backward scattered hemisphere. Their ratio for ^{181}Ta at 160 MeV is about 1.2, far less than we would expect from Fig. 10, as measured in the forward-angle region. Their ratio appears to be understood on the basis of Coulomb corrections, although Burleson *et al.*[47] have pointed out that large multiple-scattering corrections are required. It does not appear possible to compare our more forward angle data in detail

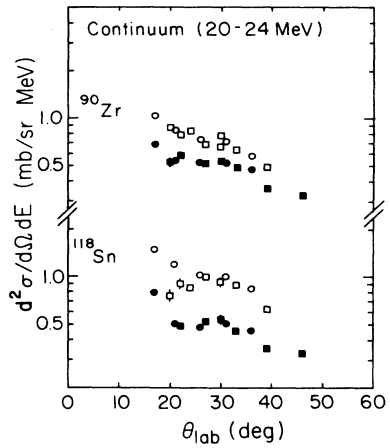

FIG. 9. Continuum cross sections averaged between 20 and 24 MeV of excitation for the low (circles) and high (squares) spectrometer field settings. A π^- enhancement is observed for both targets.

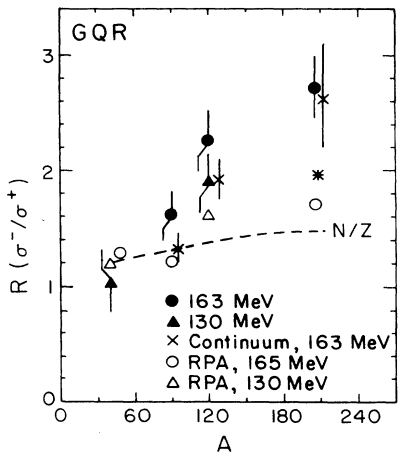

FIG. 10. Data for the ratio of the maximum differential cross sections for the GQR shown at two incident pion energies for a range of targets. For the 130 MeV data, see Ref. 1; the ^{208}Pb data at 162 MeV are from Ref. 2. Values of the ratio for the 20–24 MeV continuum are also shown. The curve represents Tassie collective·model DWIA calculations for the hydrodynamic weights of N and Z for the neutrons and protons, $M_n/M_p=N/Z$. Calculations using RPA transition densities from Ref. 45 are shown as open symbols; calculations for ^{208}Pb using RPA densities from Ref. 46 are shown as an asterisk.

with those of Ref. 48. We note, however, that the Coulomb distortions are explicitly included in our DWIA calculations.

VI. CONCLUSIONS

In this work we have compared π^- to π^+ inelastic scattering for collective excitations of two single-closed-shell nuclei. The fact that π^+ and π^- scattering can be done in the same experimental apparatus and analyzed in the same theoretical framework makes this method a particularly good probe of the neutron-proton content of the transitions. Other studies suffer from the need to compare results from different experimental probes, requiring a complete knowledge of the nuclear structure and several different reaction mechanisms.

For the first 2^+ state in ^{118}Sn, we found that $M_n/M_p \simeq N/Z$, not $M_n/M_p > N/Z$ as expected theoretically and observed with other probes. For the first 2^+ state in ^{90}Zr, we found that $M_n/M_p < N/Z$, as expected theoretically and found experimentally with other probes.

In the giant resonance region, we found that $M_n/M_p < N/Z$ for the LEOR in both Zr and Sn. However, for the GQR in both nuclei, we found that $M_n/M_p > N/Z$. If we also consider the data on the GQR in ^{208}Pb (Ref. 2) we see that this ratio deviates increasingly from N/Z with increasing A. This observation was not expected. A similar trend is also seen for the continuum immediately above the GQR in these nuclei.

One difference between the LEOR and GQR is that the LEOR is a bound state, below the neutron separation energy, while the GQR is above the neutron separation energy. Since the pion is a strongly absorbed probe, a possible explanation of the observations is an enhanced neutron transition density in the surface for the unbound states. The failure of calculations to predict the observed cross-section ratio could reflect an inadequate description of the surface region by the usual means of describing these transitions, such as a macroscopic collective transition density or an RPA transition density.

Although use of the collective model is an obvious weakness in giant resonance analyses, it is the consistency of the π^- to π^+ comparison that brings it to the forefront. Results from scattering probes that are strongly absorbed in complex nuclei should not be compared to the simple collective model reaction calculations, but in practice have always been treated in this fashion. Since heavy nuclei may have transitions neutron-rich in the surface for these unbound giant states, such strongly absorbed probes sense primarily the neutron component of the transition. Since the correct reaction calculations including these unbound features would yield larger theoretical cross sections for strongly absorbed particles, smaller fractions of the sum rule strengths would be obtained. The traditional bumps, at $65A^{-1/3}$ MeV and $80A^{-1/3}$ MeV for the GQR and nominal GMR, would therefore contain less than the transition strengths heretofore presented.

Two solutions to this situation may be considered. A correct theoretical transition density, including the correct coupling to the continuum, could be used for theoretical tests of the scattering of strongly absorbed probes. This is certain to be exquisitely sensitive to the continuum features and requires calculations extending to large radii, as pointed out in Ref. 46. A more attractive solution would be to obtain the sum-rule strengths experimentally by scattering projectiles sensitive to more than the nuclear surface. The cross section for exhausting a given fraction of the sum-rule strength is independent of the particular form of transition density, if an unweighted integration over the entire transition density is performed. Inelastic electron scattering is such a probe for the proton component, and positive kaon beams have a long nuclear mean free path and may be a suitable probe of the isoscalar component.[50] Any consistent experimental check of the isospin content of all the giant resonance transition densities is thus very difficult indeed, and it may not be possible to determine any but the proton energy-weighted sum-rule fractions if indeed the results from this pion scattering work are due to neutron binding energy considerations.

ACKNOWLEDGMENTS

We thank P. Comfort and J. R. Comfort for assistance in the data runs and J. Heisenberg for sending unpublished Fourier-Bessel coefficients for ^{90}Zr. This work was supported in part by the U.S. Department of Energy and the National Science Foundation.

[1]J. L. Ullmann, J. J. Kraushaar, T. G. Masterson, R. J. Peterson, R. S. Raymond, R. A. Ristinen, N. S. P. King, R. L. Boudrie, C. L. Morris, R. E. Anderson, and E. R. Siciliano, Phys. Rev. C **31**, 177 (1985).

[2]S. J. Seestrom-Morris, C. L. Morris, J. M. Moss, T. A. Carey, D. Drake, J. C. Douse, L. C. Bland, and G. S. Adams, Phys. Rev. C **33**, 1847 (1986).

[3]C. L. Morris *et al.*, Nucl. Instrum. Methods **A238**, 94 (1985).

[4]D. H. Youngblood, P. Bogucki, J. D. Bronson, U. Garg, Y. W. Lui, and C. M. Rozsa, Phys. Rev. C **23**, 1997 (1981).

[5]Program SAID (Scattering Analysis Interactive Dialin), R. A. Arndt and L. D. Roper (unpublished).

[6]R. A. Eisenstein and G. A. Miller, Comput. Phys. Commun. **11**, 95 (1976), modified by E. R. Siciliano (private communication).

[7]G. Rowe, M. Salomon, and R. H. Landau, Phys. Rev. C **18**, 584 (1978).

[8]S. J. Greene, C. J. Harvey, P. A. Seidl, R. Gilman, E. R. Siciliano, and M. B. Johnson, Phys. Rev. C **30**, 2003 (1984).

[9]E. Kao and S. Fallieros, Phys. Rev. Lett. **25**, 827 (1970); L. J. Tassie, Aust. J. Phys. **9**, 407 (1956).

[10]G. R. Satchler, Nucl. Phys. **A195**, 1 (1972).

[11]C. W. deJager, H. deVries, and C. deVries, At. Data Nucl. Data Tables **14**, 479 (1974).

[12]A. M. Bernstein, Adv. Nucl. Phys. **3**, 325 (1970).

[13]A. Bohr and B. R. Mottelson, *Nuclear Structure* (Benjamin, Reading, Mass, 1975), Vol. II.

[14]A. M. Bernstein, V. R. Brown, and V. A. Madsen, Phys. Lett. **103B**, 255 (1981); **106B**, 259 (1981).

[15]V.A. Madsen and V. R. Brown, Phys. Rev. Lett. **52**, 176

(1984); A. Bernstein, V. R. Brown, and V. A. Madsen, Comments Nucl. Part. Phys. **11**, 203 (1983).
[16]F. E. Bertrand, G. R. Satchler, D. J. Horen, J. R. Wu, A. D. Bacher, G. T. Emery, W. P. Jones, D. W. Miller, and A. van der Woude, Phys. Rev. C **22**, 1832 (1980).
[17]R. W. Finlay, J. Rapaport, M. H. Hadizadeh, M. Mirza, and D. E. Bainum, Nucl. Phys. **A338**, 45 (1980).
[18]T. H. Curtis *et al.*, Phys. Rev. **184**, 1162 (1969).
[19]V. R. Brown and V. A. Madsen, Phys. Rev. C **11**, 1298 (1975).
[20]R. J. Peterson, Phys. Rev. Lett. **57**, 1550 (1986).
[21]J. M. Moss, D. R. Brown, D. H. Youngblood, C. M. Rozsa, and J. D. Bronson, Phys. Rev. C **18**, 741 (1978).
[22]K. Hosoyama and Y. Torizuka, Phys. Rev. Lett. **35**, 199 (1975).
[23]S. Kailas, P. P. Singh, D. L. Friesel, C. C. Foster, P. Schwandt, and J. Wiggins, Phys. Rev. C **29**, 2075 (1984).
[24]E. J. Martens and A. M. Bernstein, Nucl. Phys. **A117**, 241 (1968).
[25]R. P. Singhal, S. W. Brain, W. A. Gillespie, A. Johnston, E. W. Lees, and A. G. Slight, Nucl. Phys. **A218**, 189 (1974).
[26]M. Lahanas *et al.*, Nucl. Phys. **A455**, 399 (1986).
[27]C. M. Rozsa, D. H. Youngblood, J. D. Bronson, Y. W. Lui, and U. Garg, Phys. Rev. C **21**, 1252 (1980).
[28]M. M. Gazzaly, N. M. Hintz, G. S. Kyle, R. K. Owen, G. W. Hoffmann, M. Bartlett, and G. Blanpied, Phys. Rev. C **25**, 408 (1982); M. M. Gazzaly, N. M. Hintz, M. A. Franey, J. Dubach, and W. C. Haxton, *ibid.* **28**, 294 (1983).
[29]N. J. DiGiacomo, R. L. Boudrie, I. Brissaud, J. J. Kraushaar, R. J. Peterson, R. A. Ristinen, E. S. Rost, and G. R. Smith, Phys. Rev. C **19**, 1132 (1979).
[30]J. Bellicard *et al.*, Nucl. Phys. **A143**, 213 (1970).
[31]D. E. Bainum, R. W. Finlay, J. Rapaport, M. H. Hadizadeh, and J. D. Carlson, Nucl. Phys. **A311**, 492 (1978).
[32]Y. Fujita, M. Fujiwara, S. Morinobu, I. Katayama, T. Yamazaki, T. Itahashi, H. Ikegami, and S. I. Hayakawa, Phys. Rev. C **32**, 425 (1985).
[33]B. Castel, G. R. Satchler, and K. Goeke, Phys. Lett. **91B**, 185 (1980).
[34]J. Heisenberg, J. Dawson, T. Milliman, O. Schwentker, J. Lichtenstadt, C. N. Papanicolas, J. Wise, J. S. McCarthy, N. Hintz, and H. P. Blok, Phys. Rev. C **29**, 97 (1984); J. Heisenberg (private communication).
[35]J. Heisenberg, in *Advances in Nuclear Physics,* edited by M. Baranger and E. Vogt (Plenum, New York, 1981), Vol. 12, p. 61.
[36]C. Olmer, D. F. Geesaman, B. Zeidman, S. Chakravarti, T. S. H. Lee, R. L. Boudrie, R. H. Siemssen, J. F. Amann, C. L. Morris, H. A. Thiessen, G. R. Burleson, J. J. Devereux, R. E. Segel, and L. W. Swenson, Phys. Rev. C **21**, 254 (1980).
[37]S. Fukuda and Y. Torizuka, Phys. Rev. Lett. **29**, 1109 (1972).
[38]J. Arvieux *et al.*, Phys. Lett. **90B**, 371 (1980).
[39]N. Marty *et al.*, Z. Phys. A **298**, 149 (1980).
[40]N. J. DiGiacomo and R. J. Peterson, Phys. Rev. C **20**, 693 (1979).
[41]R. Graetzer, S. M. Cohick, and J. X. Saladin, Phys. Rev. C **12**, 1462 (1975).
[42]T. Karapiperis and E. J. Moniz, Phys. Lett. **148B**, 253 (1984).
[43]N. Auerbach, Phys. Rev. C **27**, 1346 (1983).
[44]R. J. Peterson and J. L. Ullmann, Nucl. Phys. A **435**, 717 (1985).
[45]N. Auerbach, A. Klein, and E. R. Siciliano, Phys. Rev. C **31**, 682 (1985).
[46]R. J. Peterson and R. deHaro, Nucl. Phys. **A459**, 445 (1986).
[47]G. R. Burleson, G. S. Blanpied, J. Davis, J. S. McCarthy, R. C. Minehart, C. A. Goulding, C. L. Morris, H. A. Thiessen, W. B. Cottingame, S. Greene, C. F. Moore, W. R. Coker, J. D. Lumpe, and L. Ray, Phys. Rev. C **21**, 1452 (1980).
[48]R. D. McKeown, S. J. Sanders, J. P. Shiffer, H. E. Jackson, M. Paul, J. R. Sprecht, E. J. Stephenson, R. P. Redwine, and R. E. Segel, Phys. Rev. C **24**, 211 (1981).
[49]S. M. Levenson, D. F. Geesaman, E. P. Colton, R. J. Holt, H. E. Jackson, J. P. Schiffer, J. R. Sprecht, K. E. Stephenson, B. Zeidman, R. E. Segel, P. A. M. Gram, and C. A. Goulding, Phys. Rev. C **28**, 326 (1983).
[50]W. R. Coker, J. D. Lumpe, and L. Ray, Phys. Rev. C **31**, 1412 (1985).